

1 **Integrating Machine Learning with**
2 **Metabolic Models for Precision Trauma**
3 **Care:**
4 **Personalized Endotype Stratification**
5 **and Metabolic Target Identification:**
6 **Supplementary material 6**

7 Marin de Mas I.*^{1,2}, Moura L.³, Antunes F.L.M.³, Guerrero
8 J.M.^{4,5}, and Johansson P.I.^{1,2}

9 ¹CAG Center for Endotheliomics, Copenhagen University Hospital,
10 Rigshospitalet, 2100, Copenhagen, Denmark

11 ²Department of Clinical Medicine, Copenhagen University
12 Hospital, Rigshospitalet, 2100, Copenhagen, Denmark

13 ³Department of Electrical Engineering, Federal University of
14 Ceará, Fortaleza, 60430-160, Ceará, Brazil

15 ⁴Center for Renewable Energy and Microgrids, Huanjiang
16 Laboratory, AAU Energy, Zhejiang University, 314423, Zhejiang,
17 China

18 ⁵Center for Research on Microgrids (AAU CROM), AAU Energy,
19 Aalborg University, 9220, Aalborg , Denmark

20 **1 Methods**

21 This section describes the methodologies applied to analyze the impact of age,
22 sex and cluster of the efficiency of the simulated treatment on patients cor-
23 responding to Endotype D. The analysis includes Bayesian modeling, Markov
24 Chain Monte Carlo (MCMC) sampling, model comparison criteria (WAIC and
25 LOOIC), and prediction error evaluation using RMSE. Each subsection details
26 the mathematical basis and explains the integration of these methods in the
27 analysis. The methods applied here are implemented in Python file "Hierarchi-
28 cal_Bayesian_Analysis.py"

*Corresponding author: Marin de Mas I. Email: igor.bartolome.marin.de.mas@regionh.dk

29 **1.1 Improvement Score (IS)**

30 To quantify the degree of improvement in patients with Endotype D after sim-
31 ulating a treatment, an Improvement Score (IS) was developed. The treatment
32 simulation specifically targets the seven reactions associated with Cluster R₂,
33 as depicted in Figure 4A of the main text. The IS represents the percentage
34 improvement in terms of the expected mortality rate (EMR) that a patient
35 experiences following the simulated treatment.

36 **1.1.1 Patient Endotype Classification**

37 The classification of a patient into an endotype is based on the prediction of 600
38 features that characterize the patient’s metabolic flux profile. These features
39 are predicted using an XGBoost model and form the basis for calculating the
40 IS.

41 **1.1.2 Calculation of the Improvement Score**

42 The IS for a given patient p is calculated using the following equation:

$$\text{IS}_p = 100 \cdot \left(1 - \frac{\text{EMR}_t}{\text{EMR}_i} \right) \quad (1)$$

43 where EMR_i and EMR_t represent the initial (pre-treatment) and treated
44 (post-treatment) expected mortality rates, respectively.

45 The EMR is computed as a weighted average of mortality rates across the
46 four endotypes (A, B, C, and D) using the following formula:

$$\text{EMR} = \frac{f_A \cdot \text{mr}_A + f_B \cdot \text{mr}_B + f_C \cdot \text{mr}_C + f_D \cdot \text{mr}_D}{\sum f} \quad (2)$$

47 Here:

48 • f_A , f_B , f_C , and f_D denote the number of features for patient p classified
49 into Endotypes A, B, C, and D, respectively, by the XGBoost model.

50 • mr_A , mr_B , mr_C , and mr_D represent the observed mortality rates for En-
51 dotypes A, B, C, and D, respectively.

52 This formulation ensures that the improvement score reflects the weighted
53 contribution of the metabolic features associated with each endotype to the
54 patient’s overall expected mortality rate.

55 **1.2 Bayesian Modeling**

56 Bayesian inference provides a probabilistic framework to estimate parameters by
57 combining prior information with observed data. The method relies on Bayes’
58 theorem:

$$P(\theta|\text{data}) = \frac{P(\text{data}|\theta)P(\theta)}{P(\text{data})}, \quad (3)$$

59 where $P(\theta|\text{data})$ is the posterior distribution of the parameters θ , $P(\text{data}|\theta)$ is
60 the likelihood of the observed data given the parameters, $P(\theta)$ represents the
61 prior distribution, and $P(\text{data})$ is the evidence. For this study, we modeled the

62 improvement scores as a function of predictors such as cluster membership, age,
 63 and sex. The linear model assumed is:

$$y_i = \beta_0 + \beta_{\text{Cluster}} \cdot \text{Cluster}_i + \beta_{\text{Sex}} \cdot \text{Sex}_i + \beta_{\text{Age}} \cdot \text{Age}_i + \epsilon_i, \quad (4)$$

64 where y_i is the improvement score for observation i , β_0 is the intercept, and
 65 $\epsilon_i \sim \mathcal{N}(0, \sigma^2)$ is the error term. Non-informative priors were specified for all
 66 parameters to minimize prior biases. Bayesian models are particularly advanta-
 67 geous because they provide full posterior distributions for all parameters, allow-
 68 ing estimation of credible intervals and posterior predictive checks to evaluate
 69 the model's fit [1].

70 1.3 Markov Chain Monte Carlo (MCMC) Sampling

71 To estimate the posterior distributions of the model parameters, we used Markov
 72 Chain Monte Carlo (MCMC) sampling, specifically the No-U-Turn Sampler
 73 (NUTS), a variant of the Hamiltonian Monte Carlo algorithm. MCMC con-
 74 structs a Markov chain whose equilibrium distribution approximates the target
 75 posterior. Each iteration of the chain involves:

- 76 1. A **proposal step**, where a candidate parameter value is proposed using
 77 probabilistic rules based on the current state.
- 78 2. An **acceptance step**, where the candidate is accepted with probability:

$$\alpha = \min \left(1, \frac{P(\text{data}|\theta^*)P(\theta^*)}{P(\text{data}|\theta)P(\theta)} \right), \quad (5)$$

79 where θ^* is the proposed value and θ is the current value.

80 The NUTS sampler enhances efficiency by adaptively tuning step sizes and
 81 avoiding excessive computation. Convergence was assessed using trace plots
 82 and the Gelman-Rubin statistic [2], ensuring the chains adequately explored
 83 the posterior.

84 1.4 Model Comparison: WAIC and LOOIC

85 Model selection and comparison were performed using the Widely Applica-
 86 ble Information Criterion (WAIC) and Leave-One-Out Information Criterion
 87 (LOOIC). Both criteria evaluate model predictive accuracy while penalizing
 88 complexity.

89 **WAIC.** WAIC estimates the predictive density of new data while accounting
 90 for overfitting. It is defined as:

$$\text{WAIC} = -2 \sum_{i=1}^n \left[\log \left(\frac{1}{S} \sum_{s=1}^S P(y_i|\theta_s) \right) \right] + 2 \sum_{i=1}^n \text{Var}_{\theta} [\log P(y_i|\theta)], \quad (6)$$

91 where y_i are the observed data, $P(y_i|\theta_s)$ is the likelihood given posterior sample
 92 θ_s , and S is the number of posterior samples. Lower WAIC values indicate
 93 better model performance [3].

94 **LOOIC.** LOOIC uses cross-validation to estimate predictive accuracy by leaving out one observation at a time. It is computed as:

$$\text{LOOIC} = -2 \sum_{i=1}^n \log \left(\frac{1}{S} \sum_{s=1}^S P(y_i | \theta_s) \right). \quad (7)$$

96 We employed Pareto-smoothed importance sampling (PSIS) to efficiently approximate LOOIC [4].

98 1.5 Prediction Error Evaluation: RMSE

99 To complement WAIC and LOOIC, we computed the Root Mean Square Error
100 (RMSE) to directly evaluate prediction accuracy:

$$\text{RMSE} = \sqrt{\frac{1}{n} \sum_{i=1}^n (y_i - \hat{y}_i)^2}, \quad (8)$$

101 where y_i are the observed values, and \hat{y}_i are the predicted values. RMSE provides
102 an intuitive metric to assess how well the model predicts the observed
103 data.

104 1.6 Integration of Methods

105 These methodologies were integrated into the analytical workflow as follows:

- 106 1. **Parameter Estimation:** Bayesian modeling with MCMC provided posterior
107 distributions for all parameters, capturing uncertainty and allowing exploration of credible intervals.
- 109 2. **Model Comparison:** WAIC and LOOIC were used to compare models
110 with and without predictors (e.g., Cluster, Sex, Age) to evaluate their
111 relative contributions.
- 112 3. **Prediction Accuracy:** RMSE quantified prediction error to assess practical
113 model performance.

114 Together, these methods provided a robust framework for understanding the
115 predictors' effects on improvement scores and evaluating model performance.

116 2 Results

117 This section presents the key findings from the Bayesian hierarchical modeling
118 analysis, which explored the effects of cluster, sex, age, and their combinations
119 (e.g., sex+age, sex+cluster, age+cluster) on the observed improvement scores.
120 The results are interpreted through posterior distributions, model diagnostics,
121 and visual summaries. Due to the low number of patients with Endotype D in
122 Clusters P_1 and P_4 (2 and 6 patients, respectively), Clusters P_1 and P_2 were
123 combined into a single cluster for analysis, and the same approach was applied
124 to Clusters P_3 and P_4 . This decision is further supported by the fact that
125 Clusters P_1 and P_2 , as well as Clusters P_3 and P_4 , exhibit identical metabolic
126 flux activity profiles when the seven reactions targeted for simulating potential
127 treatment in patients with Endotype D, and corresponding to Cluster R_2 , are
128 excluded (See Figure 4A in the main text).

129 **2.1 Improvement Score Results**

130 The Improvement Score (IS) was calculated for a cohort of 41 patients whose
131 treatment was simulated by targeting the seven reactions corresponding to Clus-
132 ter R₂ (Figure 4A in the main text). Prior to the simulated treatment, all fea-
133 tures for these patients were assigned to Endotype D by the XGBoost model,
134 resulting in an initial expected mortality rate (EMR_i) of 85% for all patients.
135 Observed mortality rates for Endotypes A, B, C, and D were extracted from [5],
136 with values of 15%, 25%, 30%, and 85%, respectively.

137 Table 1 summarizes the calculated IS for each patient after the simulated
138 treatment, along with their corresponding sex, age, and cluster classification
139 (as depicted in Figure 1A). The IS, representing the percentage reduction in
140 expected mortality rate, ranged from 0% to 76.1%, with a mean IS of 18.5%.

141 The IS data will be further analyzed using a Bayesian model to assess poten-
142 tial effects of patient sex, age, and cluster membership on the observed improve-
143 ment scores. This analysis aims to identify whether these factors significantly
144 influence treatment outcomes, thereby providing insights into patient stratifica-
145 tion and personalized treatment approaches.

146 **2.1.1 Analysis of Model Parameters and Metrics**

147 Table 2 provides a summary of the parameter estimates obtained from the
148 Bayesian hierarchical model. The table includes posterior means, standard devi-
149 ations (SD), 94% highest density intervals (HDIs), effective sample sizes (ESS),
150 and *R*-hat statistics for convergence diagnostics.

151 The results of the Bayesian hierarchical model parameter estimates and
152 model comparison metrics are summarized in Table 2. Several key insights
153 can be derived from the analysis:

- 154 • **Cluster Effects:** The mean effect for **Cluster 1** (*Cluster Effect (P₁&P₂)*)
155 is 6.836 with a standard deviation (SD) of 7.859, while for **Cluster 2**
156 (*Cluster Effect (P₃&P₄)*), the mean effect is 8.657 with an SD of 5.608.
157 The 94% Highest Density Interval (HDI) for Cluster 1 ranges from -7.756
158 to 21.520, and for Cluster 2, it ranges from -2.015 to 18.922. These over-
159 lapping intervals suggest that while the posterior means indicate a positive
160 effect of cluster membership, the uncertainty is high, and statistical sig-
161 nificance cannot be established.
- 162 • **Sex Effect:** The mean effect of sex (Sex_Effect) is 7.617 (SD: 7.081), with
163 a 94% HDI spanning -5.163 to 21.479. This broad interval, crossing zero,
164 implies that there is no significant difference in outcomes based on sex.
- 165 • **Age Effect:** The effect of age (Age_Effect) shows a mean of -0.179 (SD:
166 5.788) and a 94% HDI of -11.265 to 10.617. The interval, centered around
167 zero, indicates a negligible influence of age on the outcome variable.
- 168 • **Interaction Effects:** Interactions between age, sex, and cluster member-
169 ship reveal similarly wide intervals. For instance:
 - 170 – **Age-Cluster Interaction:** The mean effects for Cluster 1 and
171 Cluster 2 are -0.215 and 0.029, respectively, with overlapping HDIs
172 (-11.552 to 10.320 and -10.122 to 11.700), suggesting minimal in-
173 teraction.

174 – **Cluster-Sex Interaction:** For Cluster 1, the mean interaction effect
175 is 10.644 (HDI: -5.449 to 25.341), while for Cluster 2, it is
176 -3.261 (HDI: -18.657 to 10.824). These trends, while intriguing,
177 are not statistically significant.

178 • **Posterior Predictive Distribution:** The posterior distributions for all
179 parameters converge appropriately, as indicated by effective sample sizes
180 (ESS_{bulk} and ESS_{tail}) exceeding 2,800 for all parameters, and the \hat{R} diag-
181 nostic being 1.0 across all estimates, confirming robust sampling.

182 • **Model Comparison and Fit:** The WAIC and LOOIC values (385.56 for
183 both) indicate similar predictive performance across the models. The Root
184 Mean Square Error (RMSE) was 33.10, highlighting the residual variabil-
185 ity in predictions. While the model captures some trends, considerable
186 uncertainty remains in the prediction of outcomes.

187 **Summary:** The analysis indicates that the effects of cluster membership
188 and sex show slight positive trends, but these trends are not statistically sig-
189 nificant given the broad credible intervals. Age, and interactions involving age,
190 appear to have negligible effects. Model diagnostics confirm adequate conver-
191 gence, but the high RMSE suggests room for improved predictive performance
192 with alternative model formulations or additional predictors.

193 2.2 Convergence Diagnostics

194 The trace plots (1A) confirm proper sampling behavior for all model param-
195 eters, including "Cluster Effect," "Sex Effect," and "Age Effect." The density
196 estimates (left panel of the trace plots) show smooth, unimodal distributions,
197 while the chains (right panel) exhibit stable mixing with no autocorrelation or
198 trends, confirming convergence to the posterior distribution. Rank plots (1D)
199 further validate convergence, showing uniformly distributed ranks across chains,
200 ensuring unbiased sampling.

201 2.3 Posterior Distributions

202 The posterior distributions of the parameters, visualized in `az.plot_posterior`,
203 provide key insights into the model:

204 • **Cluster Effect:** The posterior mean leans toward positive values (~ 0.5),
205 with a 94% highest density interval (HDI) excluding zero. This suggests a
206 positive, though not statistically conclusive, impact of cluster membership
207 on improvement.

208 • **Sex Effect:** The posterior mean is negative (~ -1), with the 94% HDI
209 also excluding zero. This implies that one sex (e.g., males or females,
210 depending on coding) may exhibit lower outcomes on average.

211 • **Age Effect:** The posterior distribution centers around zero, with wide
212 credible intervals overlapping zero, indicating no significant effect of age
213 on improvement.

214 While the credible intervals for "Cluster Effect" and "Sex Effect" suggest slight
215 trends, the overlapping intervals emphasize uncertainty and lack of conclusive
216 statistical significance.

217 **2.4 Parameter Relationships**

218 Pairwise relationships between parameters, assessed through pair plots (1C),
219 reveal weak correlations among predictors. The marginal distributions along
220 the diagonal reinforce earlier findings: "Cluster Effect" and "Sex Effect" exhibit
221 trends in their respective directions, while "Age Effect" appears centered around
222 zero with minimal impact.

223 **2.5 Model Uncertainty and Forest Plots**

224 The forest plot (1E) succinctly summarizes the posterior means and credible in-
225 tervals. Both "Cluster Effect" and "Sex Effect" show 94% HDIs that marginally
226 exclude zero, supporting observed trends but falling short of definitive evidence.
227 In contrast, the "Age Effect" shows a wide interval centered around zero, con-
228 firming its lack of significance.

229 **2.6 Posterior Predictive Checks**

230 The posterior predictive check (PPC) plot (1A) evaluates model fit. The light
231 blue bands represent predictions from the posterior, while the black line rep-
232 resents observed data. The close alignment between predicted and observed
233 means indicates that the model captures key data trends, though residual vari-
234 ability remains high. This reflects uncertainty in capturing the full variability
235 of the data, consistent with the posterior findings.

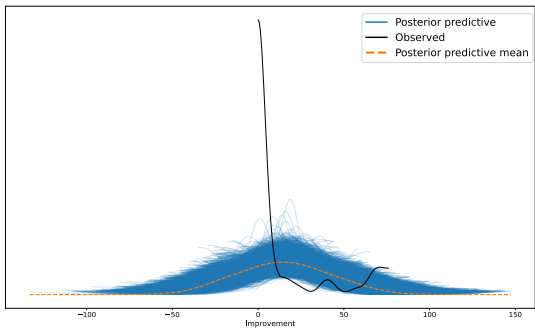
236 **2.7 Summary of Findings**

237 Based on the posterior distributions and diagnostics:

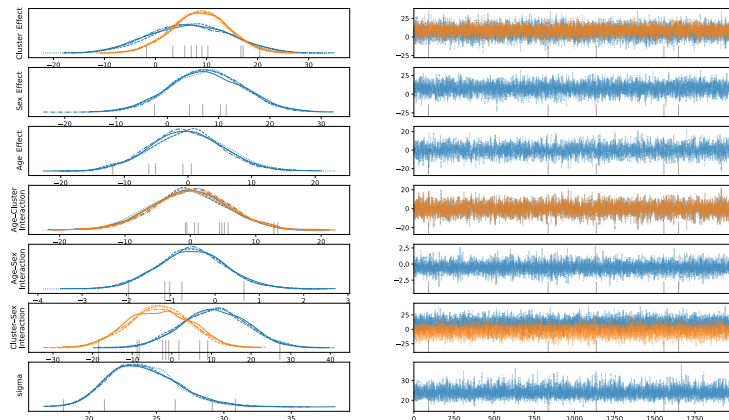
- 238 1. The **Cluster Effect** shows a positive trend, suggesting that individuals
239 in Cluster 1 may exhibit greater improvement compared to Cluster 0.
- 240 2. The **Sex Effect** indicates a negative trend, suggesting that males (or fe-
241 males, depending on coding) may experience slightly higher improvement.
- 242 3. The **Age Effect** is not significant, implying that age does not play a
243 substantial role in explaining the outcome.

244 While the trends for "Cluster Effect" and "Sex Effect" are intriguing, they are
245 not statistically conclusive due to overlapping credible intervals and residual
246 variability in the predictions.

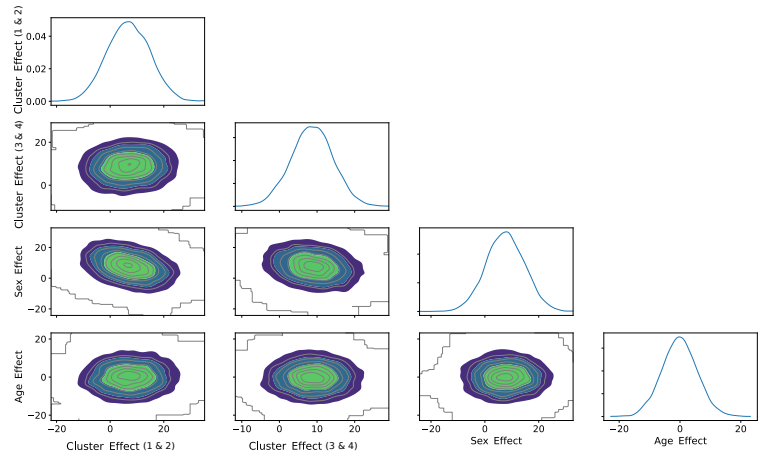
(A) Posterior Predictive Check (PPC)



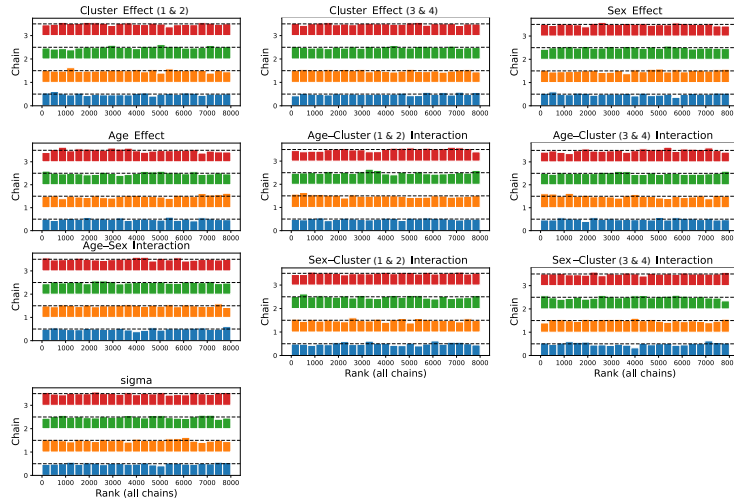
(B) Trace plot for parameters Predictive Check (PPC)



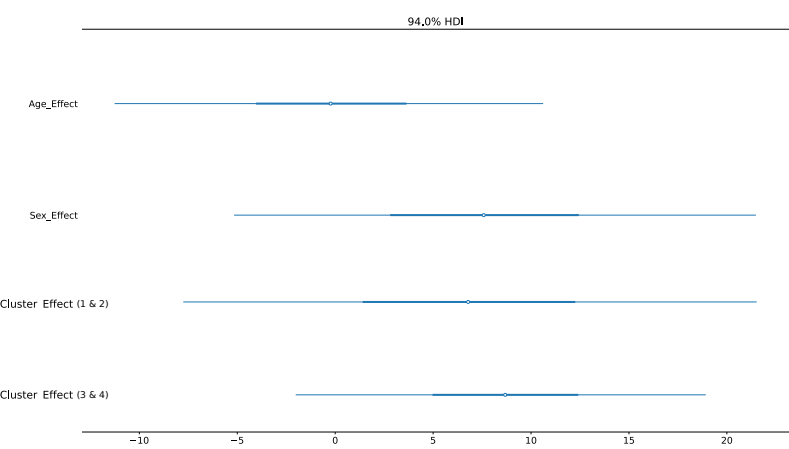
(C) Pair Plots



(D) Trace plot for parameters



(E) Density Overlay



(F) Posterior Summary Plots

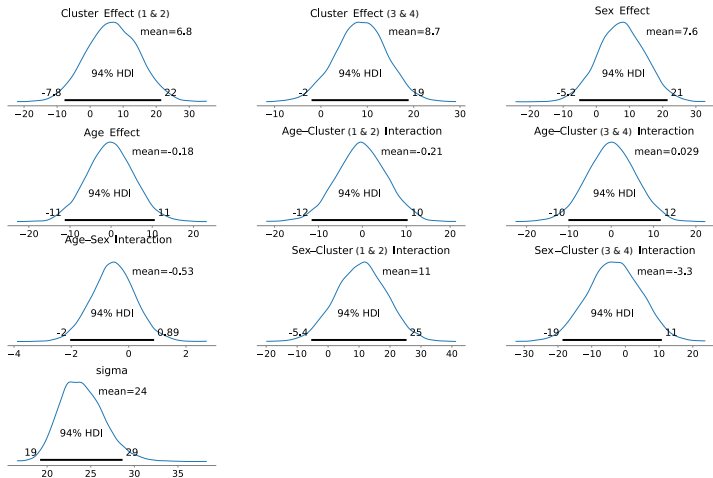


Table 1: Improvement Scores (IS) for 41 patients after simulated treatment targeting the 7 reactions in Cluster R₂. The table includes patient ID, cluster assignment, sex (1 = male, 0 = female), age, and the calculated IS, which represents the percentage reduction in expected mortality rate. The mean IS across all patients is 18.5%.

Patient ID	Cluster	Sex (1 = Male)	Age	IS (%)
4	3	0	63	0.000
5	3	1	51	37.892
6	3	1	60	0.000
10	4	0	65	40.176
12	3	1	43	0.000
13	4	0	51	0.000
15	3	1	39	72.539
17	2	1	65	0.000
22	2	1	59	0.000
24	2	1	47	13.412
25	2	1	63	76.059
26	2	1	22	68.824
27	2	1	48	66.873
28	2	0	45	0.000
32	1	1	57	0.245
33	2	1	71	0.000
35	2	1	54	65.765
44	2	1	52	0.000
46	2	1	42	7.706
47	2	1	59	4.353
54	2	0	32	0.000
55	1	1	34	56.941
57	3	0	38	0.000
60	4	1	65	0.000
65	3	0	31	70.216
66	3	1	30	2.118
67	3	0	50	43.294
68	4	1	65	2.980
69	3	1	41	18.471
72	3	1	48	15.676
74	3	1	37	6.824
75	4	1	45	0.000
78	4	1	51	0.118
81	3	1	60	0.824
83	3	0	42	0.000
84	3	0	61	2.824
87	3	0	35	0.118
88	3	1	63	2.941
89	3	1	48	0.000
91	3	1	55	24.588
92	3	0	41	0.000

Table 2: Posterior summaries of parameter estimates from the Bayesian hierarchical model, along with model comparison metrics (WAIC, LOOIC) and prediction error (RMSE). The results provide posterior means, standard deviations (SD), 94% highest density intervals (HDIs), and convergence diagnostics for key parameters.

Parameter	Mean	SD	HDI 3%	HDI 97%	MCSE Mean	MCSE SD	ESS (Bulk)	ESS (Tail)	R-hat
Cluster Effect (P_1 & P_2)	6.836	7.859	-7.756	21.520	0.106	0.079	5537.0	5618.0	1.0
Cluster Effect (P_3 & P_4)	8.657	5.608	-2.015	18.922	0.068	0.049	6825.0	5430.0	1.0
Sex Effect	7.617	7.081	-5.163	21.479	0.102	0.075	4853.0	4963.0	1.0
Age Effect	-0.179	5.788	-11.265	10.617	0.108	0.076	2877.0	3600.0	1.0
Age-Cluster Interaction (P_1 & P_2)	-0.215	5.788	-11.552	10.320	0.108	0.076	2896.0	3778.0	1.0
Age-Cluster Interaction (P_3 & P_4)	0.029	5.786	-10.122	11.700	0.107	0.076	2903.0	3583.0	1.0
Age-Sex Interaction	-0.530	0.774	-2.041	0.888	0.010	0.008	6241.0	4824.0	1.0
Cluster-Sex Interaction (P_1 & P_2)	10.644	8.289	-5.449	25.341	0.113	0.083	5392.0	5545.0	1.0
Cluster-Sex Interaction (P_3 & P_4)	-3.261	7.963	-18.657	10.824	0.108	0.082	5464.0	4531.0	1.0
σ (Error SD)	24.015	2.574	19.194	28.648	0.032	0.023	6500.0	5448.0	1.0
WAIC					385.56				
LOOIC					385.56				
RMSE					33.10				

Figure 1: Summary of Bayesian Hierarchical Model Diagnostics and Results: This figure provides a comprehensive summary of diagnostic checks and parameter estimates derived from the Bayesian hierarchical model using MCMC sampling. This figure combines diagnostic and summary visualizations to validate model convergence, assess parameter significance, and highlight key findings. (a) Posterior Predictive Check (PPC): This plot compares the observed data (black line) with posterior predictive samples (light blue bands). The close alignment of the predicted mean with the observed data indicates that the model adequately captures overall trends, although the wide predictive bands highlight residual uncertainty. (b) Trace Plots for PPC: Each row displays the trace and density plots for a model parameter (e.g., "Cluster Effect," "Sex Effect," "Age Effect"). The left panels show the smoothed posterior density estimates for the parameters, while the right panels track parameter values over MCMC iterations. Stable chains without trends or autocorrelation confirm convergence to the posterior distribution. (c) Pair Plot: This plot explores pairwise relationships between key model parameters ("Cluster Effect," "Sex Effect," and "Age Effect"). The off-diagonal 2D kernel density estimates show weak correlations, while the marginal distributions (diagonal) reinforce the distinct roles of each parameter. (d) Trace plots for parameters: These plots visualize the uniformity of rank distributions across chains for all parameters. The evenly distributed color bands indicate no sampling bias and further validate MCMC convergence. (e) Density Overlay: A succinct summary of parameter estimates, including 94% HDIs. The "Cluster Effect" and "Sex Effect" show intervals that suggest potential trends, while the "Age Effect" has wide intervals centered around zero, indicating a negligible impact. (f) Posterior Summary Plots: This plot shows the posterior distributions of key model parameters, including their means and 94% highest density intervals (HDIs). Parameters such as "Cluster Effect" and "Sex Effect" exhibit distributions leaning away from zero, while "Age Effect" centers around zero, suggesting a lack of significance.

247 3 Conclusions

248 The analysis of improvement scores using Bayesian hierarchical modeling and
 249 MCMC sampling provides the following conclusions:

250 1. No statistically significant effects were detected for **Cluster**, **Sex**, **Age**,
 251 or any combined effects (e.g., Sex+Age, Sex+Cluster, Age+Cluster). This
 252 suggests that these predictors do not strongly influence the observed out-
 253 comes in the current dataset.

254 2. Trends were observed:

255

- 256 • Individuals in **Cluster 1** tend to show slightly higher improvement
 compared to Cluster 0.
- 257 • **Males** may exhibit marginally greater improvement.

258 These trends, while not statistically significant, warrant further investiga-
 259 tion in larger datasets or with refined modeling approaches.

260 3. The **Age Effect** was found to be negligible, suggesting that age does not
261 substantially contribute to outcome variability.

262 3.1 Recommendations for Future Work

263 The lack of significant effects underscores the need for further research:

264 • Increasing the sample size could reduce credible interval widths and pro-
265 vide more robust conclusions regarding predictor effects.

266 • Incorporating additional predictors or interaction terms (e.g., non-linear
267 relationships) may help capture residual variability in the data.

268 • Targeted analysis of **Cluster** and **Sex**, given their observed trends, could
269 uncover meaningful differences with stronger evidence.

270 In conclusion, while the current analysis does not provide strong evidence
271 for significant predictor effects, the observed trends provide promising directions
272 for future investigation.

273 References

274 [1] A. Gelman et al. *Bayesian Data Analysis*. CRC Press, 2013.

275 [2] S. Brooks and A. Gelman. “General Methods for Monitoring Convergence of
276 Iterative Simulations”. In: *Journal of Computational and Graphical Statistics* 7.4 (1998), pp. 434–455.

277 [3] A. Gelman, J. Hwang, and A. Vehtari. “Understanding predictive informa-
278 tion criteria for Bayesian models”. In: *Statistics and Computing* 24 (2014),
279 pp. 997–1016.

280 [4] A. Vehtari, A. Gelman, and J. Gabry. “Practical Bayesian model evalua-
281 tion using leave-one-out cross-validation and WAIC”. In: *Statistics and*
282 *Computing* 27 (2017), pp. 1413–1432.

283 [5] H. H. Henriksen et al. “Metabolic systems analysis identifies a novel mech-
284 anism contributing to shock in patients with endotheliopathy of trauma
285 (EoT) involving thromboxane A2 and LTC4”. In: *Matrix Biology Plus* 15
286 (2022), p. 100115.